

# Phonon-induced interactions and entanglement formation between two microcavity modes mediated by two semiconductor quantum dots

J. K. Verma,<sup>1</sup> Harmanpreet Singh <sup>1</sup>, P. K. Pathak <sup>1</sup> and S. Hughes <sup>2</sup>

<sup>1</sup>Indian Institute of Technology Mandi, Mandi 175 001, Himachal Pradesh, India

<sup>2</sup>Department of Physics, Engineering Physics and Astronomy, Queen's University, Kingston, Ontario, Canada K7L 3N6



(Received 24 August 2020; accepted 2 November 2020; published 1 December 2020)

Using a polaron master equation approach, we investigate the cooperative two-photon resonance behavior between two modes of a field inside a semiconductor microcavity containing two quantum dots. The cooperative two-mode two-photon resonance occurs when two off-resonant quantum dots, initially prepared in exciton states, emit one photon in each cavity mode and deexcite simultaneously. Using this two-photon two-mode interaction, we demonstrate how to generate an entangled state of two qutrits (tripartite unit of quantum information). The bases for the qutrits are formed by the states of the cavity modes containing zero, one, and two photons. We also study the effect of exciton-phonon coupling on the entanglement and the probability of generating two-qutrit states, and explore the role of the phonon bath temperature.

DOI: [10.1103/PhysRevA.102.063701](https://doi.org/10.1103/PhysRevA.102.063701)

## I. INTRODUCTION

Semiconductor quantum dots (QDs) embedded in semiconductor microcavity systems have emerged as a new paradigm in chip-based cavity quantum electrodynamics (QED) [1,2]. Integrated QD solid-state systems have been extensively explored theoretically and experimentally in the past two decades, particularly in the quest for scalable quantum optical technology [3–7]. Various quantum optical phenomena such as enhanced exciton decay rate [8,9], vacuum Rabi splitting [10–13], Rabi oscillations [14,15], and Mollow triplets have been observed and explained [16–21].

Sources of nonclassical light such as entangled photons [22–25] and indistinguishable single photons [26,27] have also been successfully realized. Analogous to electronic states in atoms, excitons in QDs have discrete energy levels. However, QDs are semiconductor materials and one should also consider exciton-phonon interactions [28–34]. In a typical experiment, a QD embedded in a semiconductor microcavity is excited by an external field incoherently [35,36] or by using coherent pumping methods [37–40], and the fluorescence is detected either via cavity emission or through spontaneous emission decay.

While QDs can act as mesoscopic and scalable two-level systems, since they are usually embedded in a solid state environment, electron-phonon interactions are important to understand [30,31]. Signatures of phonon interactions in QDs have been clearly observed in various QD systems using optical pumping which results in exciton dephasing and cavity mode feeding in off-resonant QD-cavity interaction [41,42]. In some incoherently pumped QDs, phonon-induced off-resonant interactions with charged excitons generated during pumping and wetting-layer continuum states have been found to be partly responsible for these phenomena [43,44]. Using a quasi-resonant coherent pump, the problems associated with

unwanted transitions from charged excitons and the wetting layer do not contribute significantly and only the exciton-phonon coupling remains relevant. Moreover, the phonon interactions become more prominent in off-resonant interaction between QDs and the electromagnetic cavity fields. Therefore, off-resonant QD-cavity QED provides a platform for studying nonperturbative interactions between excitons, photons, and phonons [16–19,45–49]. Various phonon-assisted phenomena in off-resonant QDs have also been recently observed. For example, exciton and biexciton states can be prepared with high fidelity, using off-resonant pumping fields, and phonon-assisted transitions [50–55].

The steady-state population inversion from a continuous wave drive, which cannot be achieved in isolated two-level systems, has also been demonstrated in two-level QDs due to exciton-phonon coupling when the pump field is tuned above the exciton resonance [56–58]. Fast control of QD laser emission has also been demonstrated using acoustic pulses [59]. Various features due to phonon interactions have been observed in the Mollow triplet regime for off-resonant QD-cavity systems [16–21]. Most of these works have considered single QD interactions. Recently, the excitation transfer between two QDs embedded inside a photonic crystal cavity [45,46] has been predicted. The resonant interaction between two QDs and single-mode cavities has also been observed [47,60,61]. Furthermore, strong coupling between a QD molecule and a photonic crystal cavity has been investigated [62], which demonstrates tunable exciton energy and dipole coupling strengths. It was also predicted that a phonon-induced two-photon interaction can occur between two off-resonant QDs [48] interacting with a single-mode field.

In this work, we demonstrate how exciton-phonon interactions in off-resonantly coupled QDs, embedded in a bimodal microcavity, can lead to an unusual two-photon resonant

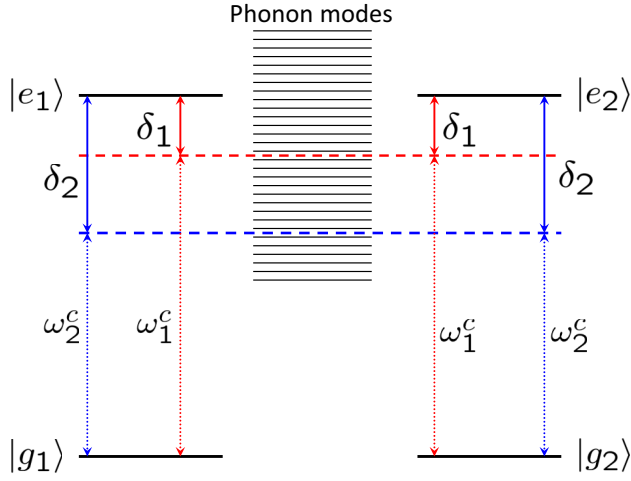


FIG. 1. Schematic energy level diagram for two separated QDs interacting with two modes of a field inside a semiconductor microcavity and with a phonon bath. We assume both QDs have the same exciton resonance frequency  $\omega_0$ . The detunings of the cavity modes with the exciton are given by  $\delta_i = \omega_0 - \omega_i^c$ .

interaction between two cavity modes. We also show how such interactions can be exploited in generating an entangled state of two photons, emitted through two cavity modes, specifically of the form

$$|\psi\rangle = \frac{1}{\sqrt{3}}(|0, 2\rangle + |1, 1\rangle + |2, 0\rangle). \quad (1)$$

Significant work has been done and has benefited from generating entangled polarization states that are described by  $|\phi\rangle = \frac{1}{\sqrt{2}}(|x_1, x_2\rangle + |y_1, y_2\rangle)$ , e.g., in a bimodal cavity through biexciton cascaded decay [49,63,64], where the labels 1 and 2 represent two modes in frequency and  $x$  and  $y$  represent two orthogonal polarizations. Here we show how one can realize the phonon-assisted generation of entangled qutrit states of two photons emitted from two cavity modes.

The rest of our paper is organized as follows. In Sec. II, we present our model for a resonant two-photon interaction between two cavity modes and develop a theoretical formalism using polaron master equation techniques [32–34]. We discuss the two-photon two-mode resonant interactions using population dynamics and the probabilities for photon emissions in Sec. III. We also study the entanglement between two modes in terms of the negativity and show its dependence on temperature in Sec. IV. Finally, we present our conclusions in Sec. V. In the Appendix, we compare results evaluated using a simplified Lindblad form of the master equation and the full polaron-transformed master equation.

## II. POLARON-TRANSFORMED MASTER EQUATION FOR TWO QDS IN A BIMODAL CAVITY

We consider two separated QDs interacting off-resonantly with two modes of a field inside a two-mode cavity as shown in Fig. 1. For simplification, we also consider exciton resonance frequencies that are the same in both QDs, with a value of  $\omega_0$ . Although it can be difficult to have two separate QDs with the same resonance frequency, there are experimental

techniques for achieving this, e.g., through tuning with magnetic fields [60] or electric fields [61].

The Hamiltonian in the rotating frame at the exciton resonance frequency is given by

$$H = -\hbar\delta_1 a_1^\dagger a_1 - \hbar\delta_2 a_2^\dagger a_2 + \hbar \sum_{i=1,2} (g_i \sigma_i^+ a_i + g'_i \sigma_i^+ a_i + \text{H.c.}) + H_{\text{phon}}, \quad (2)$$

where  $\delta_i = \omega_0 - \omega_i^c$  is the detuning between the exciton resonance and the cavity mode of frequency  $\omega_i^c$ ,  $g_i$  and  $g'_i$  are dipole coupling constants of the first and second QDs with the  $i$ th cavity mode,  $\sigma_i^+ = |e_i\rangle\langle g_i| = (\sigma_i^-)^\dagger$  is the exciton creation operator in the  $i$ th QD, and  $a_i$  is the photon annihilation operator in the  $i$ th cavity mode. Here we have not consider spontaneous emission from the QDs, which we include later in the master equation. A similar Hamiltonian for a single QD interacting with two modes has been realized in an experiment to demonstrate photon blockade [65] in a QD-cavity system, where a single QD was coupled to both horizontally and vertically polarized cavity modes due to orientation mismatch of its dipole by angle  $\theta$ .

The longitudinal acoustic phonon bath and the exciton-phonon interactions are included in the Hamiltonian term:

$$H_{\text{phon}} = \hbar \sum_k \omega_k b_k^\dagger b_k + \lambda_k \sigma_1^+ \sigma_1^- (b_k + b_k^\dagger) + \mu_k \sigma_2^+ \sigma_2^- (b_k + b_k^\dagger), \quad (3)$$

where  $\lambda_k$  and  $\mu_k$  (assumed real) are exciton-phonon coupling constants, and  $b_k$  and  $b_k^\dagger$  are annihilation and creation operators for the  $k$ th phonon mode of frequency  $\omega_k$ .

In order to treat exciton-phonon coupling nonperturbatively, we use a polaron-transformed Hamiltonian [17,32–34], defined through  $H' = e^P H e^{-P}$ , where

$$P = \sigma_1^+ \sigma_1^- \sum_k \frac{\lambda_k}{\omega_k} (b_k - b_k^\dagger) + \sigma_2^+ \sigma_2^- \sum_k \frac{\mu_k}{\omega_k} (b_k - b_k^\dagger), \quad (4)$$

which can be written as the sum of terms corresponding to the cavity-QD system, phonon-bath interactions, and system-bath interactions as  $H' = H_s + H_b + H_{sb}$ , with

$$H_s = -\hbar\Delta_1 a_1^\dagger a_1 - \hbar\Delta_2 a_2^\dagger a_2 + \langle B \rangle X_g, \quad (5a)$$

$$H_b = \hbar \sum_k \omega_k b_k^\dagger b_k, \quad (5b)$$

$$H_{sb} = \xi_g X_g + \xi_u X_u, \quad (5c)$$

where the polaron shifts  $\sum_k \lambda_k^2 / \omega_k$  and  $\sum_k \mu_k^2 / \omega_k$  are included in the effective detunings  $\Delta_1$  and  $\Delta_2$ . The system operators are given by  $X_g = \hbar \sum_{j=1,2} (g_j \sigma_j^+ a_j + g'_j \sigma_j^+ a_j) + \text{H.c.}$  and  $X_u = i\hbar \sum_{j=1,2} (g_j \sigma_j^+ a_j + g'_j \sigma_j^+ a_j) + \text{H.c.}$ , and the phonon field fluctuation operators are  $\xi_g = \frac{1}{2}(B_+ + B_- - 2\langle B \rangle)$  and  $\xi_u = \frac{1}{2i}(B_+ - B_-)$ , where  $B_\pm = \exp[\pm \sum_k \frac{\lambda_k}{\omega_k} (b_k - b_k^\dagger)] = \exp[\pm \sum_k \frac{\mu_k}{\omega_k} (b_k - b_k^\dagger)]$  are the phonon displacement operators with the expectation value  $\langle B \rangle = \langle B_+ \rangle = \langle B_- \rangle$ . The multiplication by  $\langle B \rangle$  (which is smaller than 1 for finite temperatures) in the system Hamiltonian accounts for a coherent reduction in QD-cavity couplings in the presence of phonon interactions.

We subsequently use the polaron-transformed Hamiltonian  $H'$  and the Born-Markov approximation to derive a polaron master equation for describing the dynamics of the complete system. The spontaneous emission, cavity damping, and pure dephasing are also included as Lindblad superoperators. The Lindblad superoperator corresponding to an operator  $\hat{o}$  is defined as  $\mathcal{L}[\hat{o}]\rho = \hat{o}^\dagger \hat{o} \rho - 2\hat{o} \rho \hat{o}^\dagger + \rho \hat{o}^\dagger \hat{o}$ . Note also that the background pure dephasing can account for broadening of the zero-phonon line, which typically increases with temperature [66].

The final form of master equation, in terms of the reduced density matrix for the cavity-QD coupled system,  $\rho_s$ , is written as [32]

$$\dot{\rho}_s = -\frac{i}{\hbar}[H_s, \rho_s] - \mathcal{L}_{\text{phon}}\rho_s - \sum_{i=1,2} \left( \frac{\kappa_i}{2} \mathcal{L}[a_i] + \frac{\gamma_i}{2} \mathcal{L}[\sigma_i^-] + \frac{\gamma'_i}{2} \mathcal{L}[\sigma_i^+ \sigma_i^-] \right) \rho_s, \quad (6)$$

where  $\kappa_i$  is the photon leakage rate from the  $i$ th cavity mode, and  $\gamma_i$  and  $\gamma'_i$  account for spontaneous decay and pure dephasing, respectively, for the  $i$ th QD, and

$$\mathcal{L}_{\text{phon}}\rho_s = \frac{1}{\hbar^2} \int_0^\infty d\tau \sum_{j=g,u} G_j(\tau) [X_j(t), X_j(t, \tau) \rho_s(t)] + \text{H.c.}, \quad (7)$$

where  $X_j(t, \tau) = e^{-iH_s \tau / \hbar} X_j(t) e^{iH_s \tau / \hbar}$ , and  $G_g(\tau) = \langle B \rangle^2 [\cosh(\phi(\tau)) - 1]$  and  $G_u(\tau) = \langle B \rangle^2 \sinh(\phi(\tau))$ .

The phonon bath is treated as a continuum with the spectral function  $J(\omega) = \alpha_p \omega^3 \exp[-\omega^2/2\omega_b^2]$ , where the parameters

$\alpha_p$  and  $\omega_b$  are the electron-phonon coupling and the cut-off frequency, respectively. In our calculations we use  $\alpha_p = 1.42 \times 10^{-3} g_1^2$ ,  $\omega_b = 10g_1$ , and  $g_1 = 100 \mu\text{eV}$  for InAs QDs, which gives  $\langle B \rangle = 1.0, 0.90, 0.84$ , and  $0.73$  for  $T = 0 \text{ K}, 5, 10$ , and  $20 \text{ K}$ , respectively; these values match well with recent experiments [32,67]. The phonon correlation function  $\phi(\tau)$  is given by

$$\phi(\tau) = \int_0^\infty d\omega \frac{J(\omega)}{\omega^2} \left[ \coth\left(\frac{\hbar\omega}{2k_B T}\right) \cos(\omega\tau) - i \sin(\omega\tau) \right], \quad (8)$$

where  $k_B$  and  $T$  are the Boltzmann constant and the temperature of the phonon bath, respectively.

Since we are interested in two-photon cooperative interaction between two cavity modes, we work in the condition when QDs are far off-resonant with the cavity modes, i.e., the detunings between cavity modes and the exciton resonance in QDs are much larger than their couplings ( $\Delta_1, \Delta_2 \gg g_i, g'_i$ ). Under such conditions, the master equation (6) can be further simplified, using  $H_s = -\hbar\Delta_1 a_1^\dagger a_1 - \hbar\Delta_2 a_2^\dagger a_2$ , after neglecting the terms proportional to  $g_i$  and  $g'_i$ , in the expression of  $X_j(t, \tau)$ . As a further simplification, we also consider  $g_i = g'_i$ . With this approximation, the master equation becomes of the Lindblad form which provides a more intuitive picture of the different processes involved in the ensuing dynamics.

The approximated Lindblad form of the polaron master equation (6) is given by

$$\begin{aligned} \dot{\rho}_s = & -\frac{i}{\hbar}[H_{\text{eff}}, \rho_s] - \sum_{i=1}^2 \left( \frac{\kappa_i}{2} \mathcal{L}[a_i] + \frac{\gamma_i}{2} \mathcal{L}[\sigma_i^-] + \frac{\gamma'_i}{2} \mathcal{L}[\sigma_i^+ \sigma_i^-] \right) \rho_s \\ & - \sum_{i,j,k,l=1,i \neq j}^2 \frac{\Gamma_{kl}^{--}}{2} (a_i^\dagger \sigma_j^- a_k^\dagger \sigma_i^- \rho_s - 2a_k^\dagger \sigma_i^- \rho_s a_l^\dagger \sigma_j^- + \rho_s a_l^\dagger \sigma_j^- a_k^\dagger \sigma_i^-) + \frac{\Gamma_{kl}^{++}}{2} (\sigma_j^+ a_l \sigma_i^+ a_k \rho_s - 2\sigma_i^+ a_k \rho_s \sigma_j^+ a_l + \rho_s \sigma_j^+ a_l \sigma_i^+ a_k) \\ & - \sum_{i,j,k,l=1}^2 \frac{\Gamma_{kl}^-}{2} (a_i^\dagger \sigma_j^- \sigma_i^+ a_k \rho_s - 2\sigma_i^+ a_k \rho_s a_l^\dagger \sigma_j^- + \rho_s a_l^\dagger \sigma_j^- \sigma_i^+ a_k) + \frac{\Gamma_{kl}^+}{2} (\sigma_j^+ a_l a_k^\dagger \sigma_i^- \rho_s - 2a_k^\dagger \sigma_i^- \rho_s \sigma_j^+ a_l + \rho_s \sigma_j^+ a_l a_k^\dagger \sigma_i^-), \end{aligned} \quad (9)$$

where the first term represents the effective interaction between QDs and the cavity field; the second term represents leakage from cavity modes, spontaneous decays, and pure dephasing; and the other terms represent phonon-induced cavity-QD interactions. We have assumed that background spontaneous emission rates,  $\gamma_i$ , are not affected by phonon interactions, which is a good approximation for a spectrally flat photon reservoir function (such as free space background) [68,69].

The effective Hamiltonian is given by

$$\begin{aligned} H_{\text{eff}} = & H_s - i\hbar \sum_{i,j,k,l=1}^2 \Omega_{kl}^- a_l^\dagger \sigma_j^- \sigma_i^+ a_k + \Omega_{kl}^+ \sigma_j^+ a_l a_k^\dagger \sigma_i^- \\ & - i\hbar \sum_{i,j,k,l=1,i \neq j}^2 (\Omega_{kl}^- a_l^\dagger \sigma_j^- a_k^\dagger \sigma_i^- + \text{H.c.}), \end{aligned} \quad (10)$$

where the second term contains  $\Omega_{kl}^\pm$ , which accounts for Stark shifts (for  $i = j, k = l$ ), excitation transfer between QDs (for  $i \neq j$ ), and photon transfer between cavity modes (for  $k \neq l$ ). The third term for  $k = l$  represents cooperative two-photon interaction between the two QDs and one cavity mode, and for  $k \neq l$  represents an unusual cooperative interaction between two QDs and two cavity modes. The coupling constants for these processes are as follows:

$$\begin{aligned} \Omega_{kl}^\pm &= \frac{g_k g_l}{2} \int_0^\infty d\tau (G_+ e^{\pm i\Delta_k \tau} - G_+^* e^{\mp i\Delta_l \tau}), \\ \Omega_{kl}^{--} &= \frac{g_k g_l}{2} \int_0^\infty d\tau (G_- e^{i\Delta_k \tau} - G_-^* e^{i\Delta_l \tau}), \end{aligned} \quad (11)$$

with  $G_\pm = \langle B \rangle^2 (e^{\pm\phi(\tau)} - 1)$ .

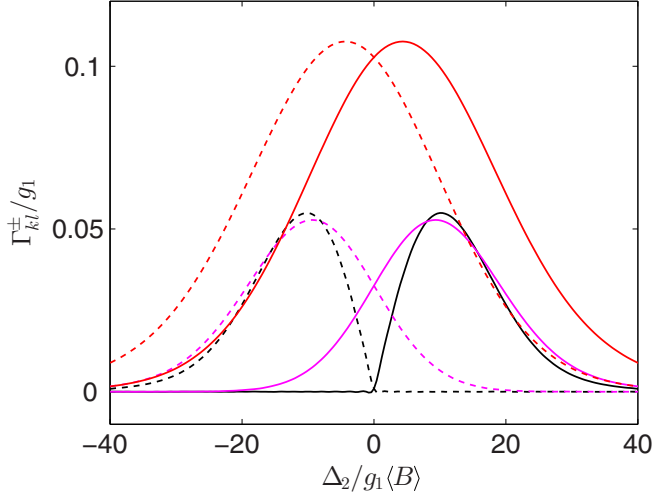


FIG. 2. Phonon-induced decay rates  $\Gamma_{kl}^-$  (dashed curves) and  $\Gamma_{kl}^+$  (solid curves) at temperatures  $T = 0$  K (black curves),  $T = 5$  K (magenta or lower gray curves), and  $T = 20$  K (red or upper gray curves). Here we use the parameters  $g_2 = g_1$  and  $\Delta_1 = \Delta_2$ ; for comparison, note that the other decay rates are  $\kappa_1 = \kappa_2 = 0.1g_1$  and  $\gamma_1 = \gamma_2 = \gamma'_1 = \gamma'_2 = 0.01g_1$ .

In Eq. (9), the rate of phonon-assisted excitation transfer between QDs and photon transfer between two modes,  $\Gamma_{kl}^\pm$ , and phonon-induced two photon processes,  $\Gamma_{kl}^{--/++}$ , are given by

$$\Gamma_{kl}^\pm = g_k g_l \int_0^\infty d\tau (G_+ e^{\pm i\Delta_k \tau} + G_+^* e^{\mp i\Delta_l \tau}), \quad (12)$$

$$\Gamma_{kl}^{--/++} = g_k g_l \int_0^\infty d\tau (G_- e^{\pm i\Delta_k \tau} + G_-^* e^{\pm i\Delta_l \tau}), \quad (13)$$

where  $\Gamma_{kl}^{--}$  and  $\Gamma_{kl}^{++}$  are complex and may not represent two-photon transition rates exactly. However, they satisfy  $\Gamma_{kl}^{--} = (\Gamma_{lk}^{++})^*$  and appear with Hermitian conjugate terms.

Numerically we solve the master equation (6) using the quantum optics toolbox in MATLAB [70]. The results obtained from the approximate Lindblad form of the master equation (9) and the full polaron master equation (6) match reasonably well. We relegate further details to the Appendix.

### III. COOPERATIVE TWO-MODE TWO-PHOTON INTERACTION

In order to maximally exploit a phonon-induced two-photon interaction between two cavity modes, we consider QDs that are off-resonantly coupled with the cavity modes. Due to the form of the phonon spectral density,  $J(\omega)$ , there is a peak in the phonon density of states at around 1 meV away from the zero-phonon line, and thus the phonon-induced transitions are more pronounced in this region. In order to understand the behavior of phonon-induced decay rates, we plot  $\Gamma_{kl}^\pm$  at different temperatures,  $T = 0, 5,$  and  $20$  K, in Fig. 2. Clearly for the temperature range 5–20 K, and  $|\Delta_i| \approx 5g_1$ , the phonon-induced decay rates are significant in comparison to other decay rates in the cavity-QED system. As expected, we also notice an asymmetry between  $\Gamma_{kl}^+$  and  $\Gamma_{kl}^-$ , which is more pronounced at lower temperatures. Further, at  $T = 0$  K,

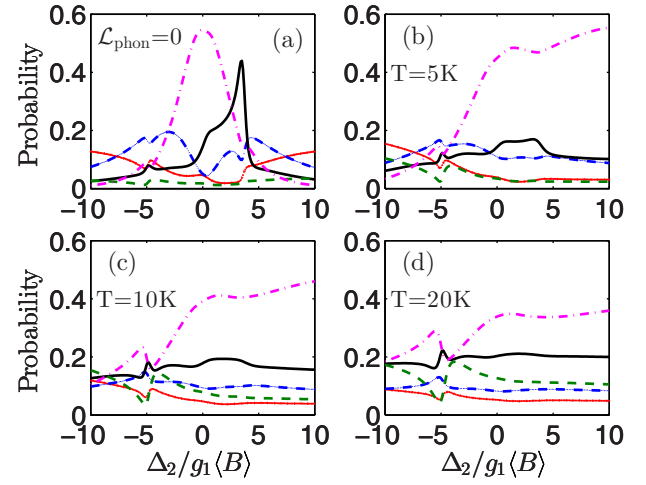


FIG. 3. Photon emission probabilities from the cavity modes, with a negative QD-cavity detuning ( $\Delta_1$ ):  $P_{10}$  from state  $|g_1, e_2, 1, 0\rangle$  (red marked dotted curves),  $P_{01}$  from state  $|g_1, e_2, 0, 1\rangle$  (blue marked dashed curves),  $P_{20}$  from state  $|g_1, g_2, 2, 0\rangle$  (green dashed curves),  $P_{02}$  from state  $|g_1, g_2, 0, 2\rangle$  (magenta dot-dashed line), and  $P_{11}$  from state  $|g_1, g_2, 1, 1\rangle$  (black solid curves). In panel (a), the exciton-phonon interactions are switched off and in panels (b)–(d) we include exciton-phonon interactions at different temperatures. The main parameters are  $g_2 = 1.5g_1$ ,  $\Delta_1 = -5g_1(B)$ ,  $\kappa_1 = \kappa_2 = 0.1g_1$ , and  $\gamma_1 = \gamma_2 = \gamma'_1 = \gamma'_2 = 0.01g_1$ .

$\Gamma_{kl}^+$  ( $\Gamma_{kl}^-$ ) is zero for negative (positive) detunings, indicating phonon-assisted transitions in QDs associated with phonon absorption are negligible at very low temperatures.

In Figs. 3 and 4, we consider different cavity mode coupling strengths with  $g_1 \neq g_2$ , while in Figs. 6 and 7 we consider  $g_1 = g_2$ . Initially the QD-cavity system is in state  $|e_1, e_2, 0, 0\rangle$ ; i.e., both QDs are in the exciton state and there are no photons in the cavity modes. We plot the photon emission probabilities, including

$$P_{10} = \kappa_1 \int_0^\infty \langle g_1, e_2, 1, 0 | \rho_s(t') | g_1, e_2, 1, 0 \rangle dt', \quad (14)$$

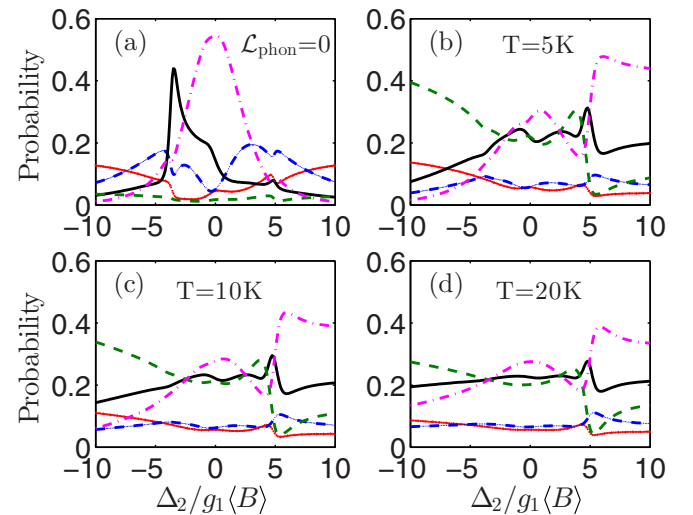


FIG. 4. Calculations similar to those in Fig. 3, except  $\Delta_1 = 5g_1(B)$  (positive QD-cavity detuning).

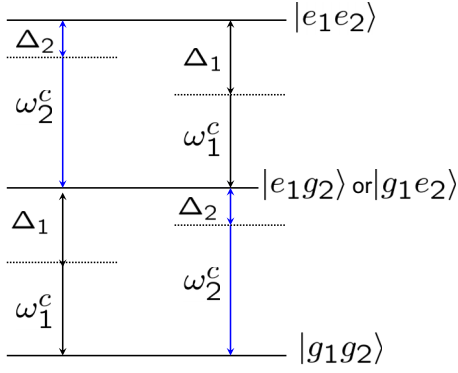


FIG. 5. Schematic energy level diagram for two-photon transitions from the exciton states when one photon is emitted in each of the cavity modes. There are two possible paths when the first photon is emitted in the first mode or in the second mode.

from state  $|g_1, e_2, 1, 0\rangle$ , and

$$P_{01} = \kappa_2 \int_0^\infty \langle g_1, e_2, 0, 1 | \rho_s(t') | g_1, e_2, 0, 1 \rangle dt', \quad (15)$$

from state  $|g_1, e_2, 0, 1\rangle$ , which are equal to the photon emission probabilities from states  $|e_1, g_2, 1, 0\rangle$  and  $|e_1, g_2, 0, 1\rangle$ , respectively. We also plot photon emission probabilities from two-photon states, defined through

$$P_{20} = 2\kappa_1 \int_0^\infty \langle g_1, g_2, 2, 0 | \rho_s(t') | g_1, g_2, 2, 0 \rangle dt', \quad (16)$$

$$P_{02} = 2\kappa_2 \int_0^\infty \langle g_1, g_2, 0, 2 | \rho_s(t') | g_1, g_2, 0, 2 \rangle dt', \quad (17)$$

$$P_{11} = (\kappa_1 + \kappa_2) \int_0^\infty \langle g_1, g_2, 1, 1 | \rho_s(t') | g_1, g_2, 1, 1 \rangle dt', \quad (18)$$

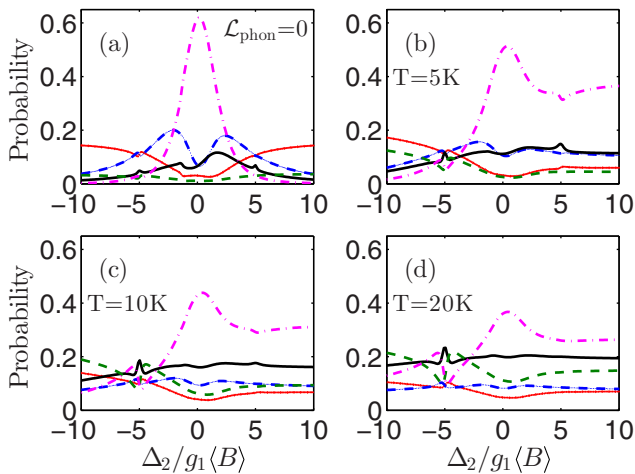


FIG. 6. Photon emission probabilities from the cavity modes:  $P_{10}$  from state  $|g_1, e_2, 1, 0\rangle$  (red marked dotted curves),  $P_{01}$  from state  $|g_1, e_2, 0, 1\rangle$  (blue marked dashed curves),  $P_{20}$  from state  $|g_1, g_2, 2, 0\rangle$  (green dashed curves),  $P_{02}$  from state  $|g_1, g_2, 0, 2\rangle$  (magenta dot-dashed curves), and  $P_{11}$  from state  $|g_1, g_2, 1, 1\rangle$  (black solid curves). The parameters are  $g_2 = g_1$ ,  $\Delta_1 = -5g_1\langle B \rangle$ ,  $\kappa_1 = \kappa_2 = 0.1g_1$ , and  $\gamma_1 = \gamma_2 = \gamma'_1 = \gamma'_2 = 0.01g_1$ .

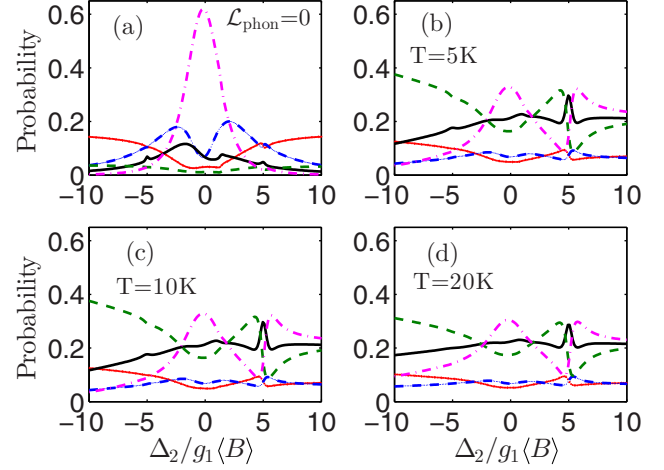


FIG. 7. Photon emission probabilities from the cavity modes:  $P_{10}$  from state  $|g_1, e_2, 1, 0\rangle$  (red marked dotted curves),  $P_{01}$  from state  $|g_1, e_2, 0, 1\rangle$  (blue marked dashed curves),  $P_{20}$  from state  $|g_1, g_2, 2, 0\rangle$  (green dashed curves),  $P_{02}$  from state  $|g_1, g_2, 0, 2\rangle$  (magenta dot-dashed curves), and  $P_{11}$  from state  $|g_1, g_2, 1, 1\rangle$  (black solid curves). The parameters are the same as those in Fig. 6, except  $\Delta_1 = 5g_1\langle B \rangle$ .

from states  $|g_1, g_2, 2, 0\rangle$ ,  $|g_1, g_2, 0, 2\rangle$ , and  $|g_1, g_2, 1, 1\rangle$ , respectively.

In Fig. 3, we fix the detuning of the first cavity mode from exciton resonances to  $\Delta_1 = -5g_1\langle B \rangle$ , and we scan the detuning of the second cavity mode,  $\Delta_2$ , to explore the two-photon two-mode resonance. In Fig. 3(a), when the phonon interactions are absent, the probability of photon emission  $P_{02}$  from state  $|g_1, g_2, 0, 2\rangle$  has an almost symmetric bell shape, with a peak at  $\Delta_2 = 0$ , which reflects that when the second mode is resonant with both QDs the cooperative emission in state  $|g_1, g_2, 0, 2\rangle$  is dominant; this regime leads to hyper-radiant [71] behavior in a high-quality cavity, where two atoms coupled to a single-mode cavity can exceed the free-space super-radiant behavior. For positive values of  $\Delta_2$ , the probability  $P_{11}$  starts to dominate and has a peak at  $\Delta_2 = 3.5g_1$  which indicates the resonant two-mode cooperative transitions from state  $|e_1, e_2, 0, 0\rangle$  to state  $|g_1, g_2, 1, 1\rangle$ , where both excitons decay simultaneously after emitting one photon in each cavity mode. The resonance condition is given by  $\Delta_1 + \Delta_2 + 2g_1^2/\Delta_1 + 2g_2^2/\Delta_2 \approx 0$ , i.e., when the sum of the frequencies of the cavity modes is equal to the sum of the exciton frequencies including Stark shifts. Note also that the probability  $P_{20}$  remains negligible for all values of  $\Delta_2$ , indicating weak transition to state  $|g_1, g_2, 2, 0\rangle$ . The photon emission probabilities  $P_{10}$  and  $P_{01}$  from states  $|g_1, e_2, 1, 0\rangle$  and  $|g_1, e_2, 0, 1\rangle$  also remain low and show spectral dips when two-photon transitions in cavity modes are dominating.

In Figs. 3(b)–3(d), we introduce coupling with a phonon bath at temperatures  $T = 5, 10$ , and  $20$  K, respectively. In the presence of phonon interactions, the peak at  $\Delta_2 = 3.5g_1$  in the probability  $P_{11}$ , corresponding to resonant two-mode two-photon transitions when one photon is emitted in each cavity mode, disappears; this is due to the fact that the transition paths, corresponding to first photon emitted in the first mode or in the second mode, become distinguishable

due to the frequency difference between phonons involved in facilitating these off-resonant transitions. The phonons having frequencies close to the detunings are involved in phonon-assisted two-photon transitions as shown in Fig. 5. As a result the constructive interference responsible for two-mode two-photon resonant interaction diminishes. However, the probability  $P_{02}$  dominates for positive values of detuning,  $\Delta_2$ , due to the enhanced two-photon interaction with the second mode followed by phonon emission in the bath at low temperature [48]. On increasing the bath temperature, an enhancement for two-photon interactions between single-mode two-QD and two-mode two-QD for negative values of  $\Delta_2$  also occurs. For  $\Delta_2 = \Delta_1$ , a small resonance peak appears in  $P_{11}$  where  $P_{02}$  and  $P_{20}$  follow a dip, showing phonon-induced resonant two-mode two-photon transition to state  $|g_1, g_2, 1, 1\rangle$ . The phonon-assisted two-photon transitions in single-mode and two-modes are not significantly large for negative detunings. The probabilities  $P_{10}$  and  $P_{01}$  remain small, indicating small emission probabilities from individual QDs. It has been observed experimentally that  $\gamma'$  increases as a function of temperature [66]. However, our results are not very sensitive to small values of pure dephasing rates  $\gamma'_i$ ; therefore, we have considered a constant value for the dephasing rates.

In Fig. 4, we now change the detuning from the first cavity mode to a fixed *positive* value of  $\Delta_1 = 5g_1\langle B\rangle$ . As expected, without phonon interactions, Fig. 4(a) is the mirror image of Fig. 3(a). However, when the interaction with the phonon bath is considered at  $T = 5$  K, in Fig. 4(b), the probability  $P_{20}$  dominates for negative values of  $\Delta_2$ . For positive values of  $\Delta_2 > 5g_1$ , the probability  $P_{02}$  dominates, indicating an enhanced two-photon transition in the second mode. Furthermore,  $\Delta_2$  on increasing  $\Delta_2$ , the probability  $P_{20}$  decreases and the probabilities  $P_{11}$  and  $P_{02}$  increase. For  $\Delta_1 \approx \Delta_2$ , the probabilities  $P_{20}$  and  $P_{02}$  corresponding to two-photon transitions in individual cavity modes are equal and follow a minimum feature, whereas the probability  $P_{11}$  corresponding to phonon-assisted cooperative two-mode two-photon transitions has a resonance peak. On increasing the phonon bath temperature, in Figs. 4(c) and 4(d), the two-photon transitions with phonon absorption are enhanced, and thus the probabilities  $P_{02}$  and  $P_{11}$  increase for negative values of  $\Delta_2$ . The probabilities  $P_{10}$  and  $P_{01}$  corresponding to emission from individual QDs remain very small. It is clear that by changing the detuning with the second cavity mode  $\Delta_2$ , one can change the nature of the interactions of the first cavity mode.

Next, in Figs. 6 and 7, we consider equal dipole coupling strengths with both cavity modes  $g_1 = g_2$ , but set  $\Delta_1 = -5g_1\langle B\rangle$  and  $\Delta_1 = 5g_1\langle B\rangle$ , respectively. We observe from Figs. 6(a) and 7(a) that, in the absence of phonon interactions, the resonance peak in probability  $P_{11}$  corresponding to cavity-induced two-mode two-photon interaction is negligible. In Figs. 6(b), 6(c), and 6(d), the probability  $P_{02}$  has a peak at  $\Delta_2 = 0$  corresponding to hyper-radiant behavior and dominates for positive values of  $\Delta_2$ , indicating phonon-assisted off-resonant interactions contribute significantly for positive detuning. Moreover, in Figs. 6(b), 6(c), and 6(d), when the temperature of the phonon bath increases from 5 to 20 K, the probabilities  $P_{11}$  and  $P_{20}$  increase. There is also a small resonance peak in  $P_{11}$  at  $\Delta_2 = \Delta_1$ , corresponding to phonon-

induced two-mode two-photon resonance which grows upon increasing temperature as the phonon absorption probability increases. However the peak at  $\Delta_2 = -\Delta_1$ , corresponding to cavity-induced two-mode two-photon emission, disappears as the which-path information gets imprinted on the phonon bath. The effects on positive detunings are associated with the absorption of phonons, and effects on negative detunings are associated with the emission of phonons.

In Fig. 7, for negative values of  $\Delta_2$ , similar to Fig. 4, the probability  $P_{20}$  dominates. When the detuning  $\Delta_2$  increases,  $P_{02}$  and  $P_{11}$  increase and  $P_{02}$  dominates for  $\Delta_2 = 0$  which decreases up to  $\Delta_2 = \Delta_1$  where  $P_{20}$  also has a minima and  $P_{11}$  has a peak corresponding to phonon-assisted two-mode two-photon resonance. From the above discussions, we find that when the detunings from the first cavity mode and second cavity mode,  $\Delta_1$  and  $\Delta_2$ , are both negative, the probabilities of single-mode two-photon transition and two-mode two-photon transition remain small. However, when both  $\Delta_1$  and  $\Delta_2$  are positive, a single-mode two-photon transition and two-mode two-photon transitions dominate. Moreover, for  $\Delta_1 = \Delta_2$ , the two-mode two-photon transition is the dominating resonance. Since these two-photon transitions are facilitated by phonons, on increasing temperature the transition probabilities also increase. For higher temperatures, the two-mode two-photon transition becomes almost independent of the detuning  $\Delta_2$ , except at resonance  $\Delta_1 = \Delta_2$ , which reflects the fact that at higher temperatures the transitions facilitated by phonon absorption or emission are almost equally probable.

#### IV. ENTANGLEMENT BETWEEN TWO CAVITY MODES

When both photons are emitted from the cavity modes, the number of photons emitted from each cavity mode forms the basis of a qutrit [72]. The state of the emitted photons at time  $t$  can be described as

$$|\psi(t, \tau)\rangle \sim \{a_1^\dagger(t)a_1^\dagger(t + \tau) + a_1^\dagger(t)a_2^\dagger(t + \tau) + a_2^\dagger(t)a_2^\dagger(t + \tau)\}|0, 0\rangle, \quad (19)$$

where  $\tau$  is delay time between photons and state  $|0, 0\rangle$  is the two-mode vacuum state.

To reconstruct the density matrix of photons emitted from the cavity modes, coincidence measurements can be performed. The photon coincidence measurements are given by two time correlation functions  $G_{ij,kl}^{(2)}(t, \tau) = \langle a_i^\dagger(t)a_j^\dagger(t + \tau)a_k(t + \tau)a_l(t) \rangle$ , where  $t$  and  $\tau$  are, respectively, the time of arrival of the first photon at the detector and the delay time for the second photon; indices  $i, j, k$ , and  $l$  correspond to the mode that each photon is emitted from. If both photons are emitted from the same cavity mode  $i = j$  ( $k = l$ ), then the only nonzero density matrix elements of two photons emitted through two modes can be reconstructed [73,74] as follows:

$$\rho_{20,11} \propto \int_0^\infty dt \int_{-\infty}^\infty d\tau G_{11,12}^{(2)}(t, \tau), \quad (20a)$$

$$\rho_{20,02} \propto \int_0^\infty dt \int_{-\infty}^\infty d\tau G_{11,22}^{(2)}(t, \tau), \quad (20b)$$

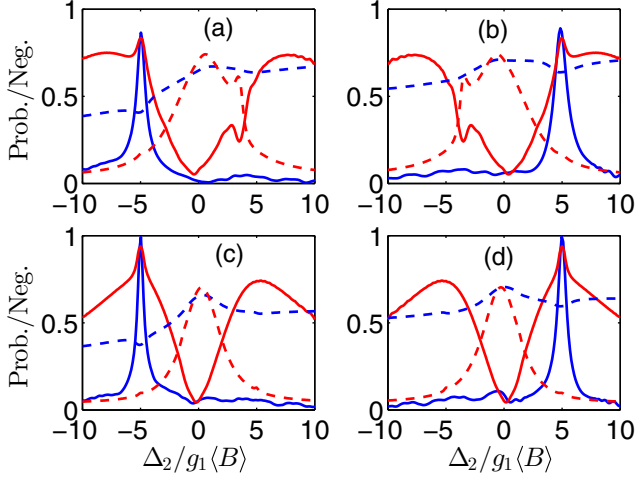


FIG. 8. The probability of generation (dashed curve) and the negativity (solid curve) for the entangled two-photon state, emitted through two modes when exciton-phonon interactions are switched off (red or gray lines) and including exciton-phonon interactions at  $T = 10$  K (blue or dark curves). In panel (a) we use the same parameters as in Fig. 3, in panel (b), we use the same parameters as in Fig. 4, in panel (c) we use the same parameters as in Fig. 6, and in panel (d) we use the same parameters as in Fig. 7.

$$\rho_{11,02} \propto \int_0^\infty dt \int_{-\infty}^\infty d\tau G_{12,22}^{(2)}(t, \tau), \quad (20c)$$

$$\rho_{20,20} \propto \int_0^\infty dt \int_{-\infty}^\infty d\tau G_{11,11}^{(2)}(t, \tau), \quad (20d)$$

$$\rho_{02,02} \propto \int_0^\infty dt \int_{-\infty}^\infty d\tau G_{22,22}^{(2)}(t, \tau), \quad (20e)$$

$$\rho_{11,11} \propto \int_0^\infty dt \int_{-\infty}^\infty d\tau G_{12,21}^{(2)}(t, \tau). \quad (20f)$$

In order to quantitatively characterize the entanglement between the two cavity modes, we calculate the negativity for the entangled state of the emitted photons. The negativity is defined as the absolute value of the sum of the negative eigenvalues of the partially transposed density matrix [75]. The partially transposed density matrix  $\rho_{kj,il}^T = \rho_{ij,kl}$  has negative eigenvalues:  $-|\rho_{20,11}|$ ,  $-|\rho_{20,02}|$ , and  $-|\rho_{11,02}|$ . The negativity for the state (19) is given by

$$\mathcal{N} = \frac{|\rho_{20,11}| + |\rho_{20,02}| + |\rho_{11,02}|}{|\rho_{20,20}| + |\rho_{02,02}| + |\rho_{11,11}|}, \quad (21)$$

where the denominator is required for normalization.

In Fig. 8, we show the probability of generating an entangled two-qutrit state and negativity without exciton-phonon interactions and with exciton-phonon interactions at  $T = 10$  K using the same parameters as in Figs. 3 and 4 and Figs. 6–7. In the absence of phonon interactions the probability of generating entangled two-qutrit states and negativity are shown with red (gray) dashed and solid curves. We find that the probability of generating two entangled qutrits is maximum around  $\Delta_2 = 0$ , where the generation of the two-photon state  $|g_1, g_2, 0, 2\rangle$  dominates and gradually decreases on increasing  $|\Delta_2|$ . In the case of asymmetric dipole couplings,

$g_1 \neq g_2$ , shown in Fig. 8(a) and 8(b), at the cavity-induced two-photon two-mode resonance it also has a larger value where the generation of the two-photon state  $|g_1, g_2, 1, 1\rangle$  dominates. The maximum probability of generating entangled qutrits remains around 0.7 due to photon losses from spontaneous decay of one or both excitons and photon emission from states  $|e_1, g_2, 1, 0\rangle$ ,  $|e_1, g_2, 0, 1\rangle$ ,  $|g_1, e_2, 1, 0\rangle$ , and  $|g_1, e_2, 0, 1\rangle$ . On the other hand, the negativity is maximum for  $\Delta_1 = \Delta_2$ , when the emitted photons match in frequency. It is clear that the probability of generating an entangled two-qutrit is negligible when the negativity is maximum in the absence of phonon interactions.

Finally, we discuss the probability of generating entangled two-qutrit states and negativity after including phonon interactions at  $T = 10$  K with blue (dark) dashed and solid curves, respectively (Fig. 8). We find that photons are maximally entangled for  $g_1 = g_2$  and  $\Delta_1 = \Delta_2$ , and the negativity drops to zero for  $\Delta_2 \neq \Delta_1$ , since which-path information is revealed by the phonons involved in facilitating off-resonant transitions when the cavity modes have different detunings. Furthermore, for  $g_1 = g_2$ , the spectra of emitted photons from both modes overlap perfectly which makes both modes maximally entangled. The probability of generating a two-qutrit entangled state is larger than 0.6 for positive detunings and is smaller than 0.4 for negative detunings because of the asymmetric nature of phonon-induced two-mode two-photon interactions at lower temperatures. Therefore, for the parameters used in Figs. 4 and 7, one can indeed generate highly entangled two-mode two-photon states using phonon-assisted two-mode two-photon interactions. After the entangled photon pair is generated, the lifetime of entanglement depends on noise in the channel it propagates. It has been observed that, in bipartite-entangled photonic states, entangled qutrits are less susceptible to noise than entangled qubits [76].

In the context of currently available technologies, experiments have been performed for two QDs coupled to a mode of photonic crystal cavity [45–47,60,61] and a micropillar cavity [77,78]. In addition, experiments with single QDs coupled with two cavity modes have also been performed successfully [65,79,80]. There are also various techniques developed for tuning exciton and cavity mode frequencies for resonant coupling [60,61]. Thus, an exploration of coupled QDs with two modes of a semiconductor microcavity can be realized experimentally.

## V. CONCLUSIONS

Using a polaronic master equation to describe interactions between two QDs, two cavity modes, and phonons, we have predicted large phonon-assisted two-mode two-photon interactions in the system of two off-resonantly coupled QDs inside a bimodal semiconductor cavity. We have found that the cavity field induces two-mode two-photon resonances, which appear for  $g_1 \neq g_2$ , and are strongly suppressed in the presence of exciton-phonon interactions, and the phonon-assisted two-mode two-photon resonances occur at  $\Delta_1 = \Delta_2$ . Furthermore, these interactions are more pronounced for positive detunings. Our results could help open up an alternative way for generating entangled two-mode qutrit states from chip-based QD-cavity systems.

## ACKNOWLEDGMENTS

This work was supported by Department of Science and Technology, India, SERB Fast Track Young Scientist Scheme SR/FTP/PS-122/2011, Queen's University, Canada, the Canadian Foundation for Innovation, and the Natural Sciences and Engineering Research Council of Canada.

APPENDIX: COMPARISON BETWEEN THE SIMPLIFIED POLARON MASTER EQ. (9) AND THE FULL POLARON-TRANSFORMED MASTER EQ. (6)

In order to check the validity of the simplified polaronic master equation (9), in Fig. 9 we also compare photon emission probabilities from cavity modes calculated using the polaron-transformed master equation (6), for the same parameters as in Fig. 7(c). The results match reasonably well, indicating that the simplified master equation captures the main physics behind different phonon-assisted processes in the two-QD two-mode interaction regime. Similarly matching results using the simplified master equation are found for other parameters used in Figs. 3–7 (not shown).

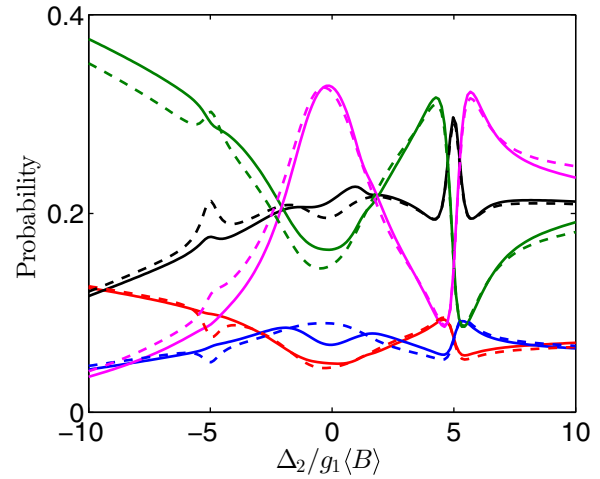


FIG. 9. Photon emission probabilities from the two cavity modes,  $P_{10}$  from state  $|g_1, e_2, 1, 0\rangle$  (red curve),  $P_{01}$  from state  $|g_1, e_2, 0, 1\rangle$  (blue curve),  $P_{20}$  from state  $|g_1, g_2, 2, 0\rangle$  (green curve),  $P_{02}$  from state  $|g_1, g_2, 0, 2\rangle$  (magenta curve), and  $P_{11}$  from state  $|g_1, g_2, 1, 1\rangle$  (black curve). The parameters are the same as those in Fig. 7(c). The dashed curves correspond to the simplified polaronic master equation (9), and the solid curves correspond to the full polaron-transformed master equation (6).

- [1] A. Kiraz, C. Reese, B. Gayral, L. Zhang, W. V. Schoenfeld, B. D. Gerardot, P. M. Petroff, E. L. Hu, and A. Imamoglu, *J. Opt. B: Quantum Semiclass. Opt.* **5**, 129 (2003).
- [2] J. Vučković and Y. Yamamoto, *Appl. Phys. Lett.* **82**, 2374 (2003).
- [3] A. Faraon, A. Majumdar, D. Englund, E. Kim, M. Bajcsy, and J. Vučković, *New J. Phys.* **13**, 055025 (2011).
- [4] S. Sun, H. Kim, Z. Luo, G. S. Solomon, and E. Waks, *Science* **361**, 57 (2018).
- [5] H.-R. Wei and F.-G. Deng, *Sci. Rep.* **4**, 7551 (2014).
- [6] M. Davanco, J. Liu, L. Sapienza, C.-Z. Zhang, J. Vinfcius De Miranda Cardoso, V. Verma, R. Mirin, S. W. Nam, L. Liu, and K. Srinivasan, *Nat. Commun.* **8**, 889 (2017).
- [7] P. Lodahl, S. Mahmoodian, and S. Stobbe, *Rev. Mod. Phys.* **87**, 347 (2015).
- [8] F. Liu, A. J. Brash, J. O'Hara, L. M. P. P. Martins, C. L. Phillips, R. J. Coles, B. Royall, E. Clarke, C. Bentham, N. Ptrljaga, I. E. Itskevich, L. R. Wilson, M. S. Skolnick, and A. Mark Fox, *Nat. Nanotechnol.* **13**, 835 (2018).
- [9] M. D. Birowosuto, H. Sumikura, S. Matsuo, H. Taniyama, P. J. van Veldhoven, R. Nötzel, and M. Notomi, *Sci. Rep.* **2**, 321 (2012).
- [10] G. Khitrova, H. M. Gibbs, M. Kira, S. W. Koch, and A. Scherer, *Nat. Phys.* **2**, 81 (2006).
- [11] T. Yoshie, A. Scherer, J. Hendrickson, G. Khitrova, H. M. Gibbs, G. Rupper, C. Ell, O. B. Shchekin, and D. G. Deppe, *Nature (London)* **432**, 200 (2004).
- [12] Y. Ota, D. Takamiya, R. Ohta, H. Takagi, N. Kumagai, S. Iwamoto, and Y. Arakawa, *Appl. Phys. Lett.* **112**, 093101 (2018).
- [13] Y. Ota, R. Ohta, N. Kumagai, S. Iwamoto, and Y. Arakawa, *Phys. Rev. Lett.* **114**, 143603 (2015).
- [14] T. H. Stievater, X. Li, D. G. Steel, D. Gammon, D. S. Katzer, D. Park, C. Piermarocchi, and L. J. Sham, *Phys. Rev. Lett.* **87**, 133603 (2001).
- [15] K. Kuruma, Y. Ota, M. Kakuda, S. Iwamoto, and Y. Arakawa, *Phys. Rev. B* **97**, 235448 (2018).
- [16] A. Majumdar, E. D. Kim, Y. Gong, M. Bajcsy, and J. Vučković, *Phys. Rev. B* **84**, 085309 (2011).
- [17] C. Roy and S. Hughes, *Phys. Rev. Lett.* **106**, 247403 (2011).
- [18] A. Ulhaq, S. Weiler, C. Roy, S. M. Ulrich, M. Jetter, S. Hughes, and P. Michler, *Opt. Express* **21**, 4382 (2013).
- [19] R.-C. Ge, S. Weiler, A. Ulhaq, S. M. Ulrich, M. Jetter, P. Michler, and S. Hughes, *Opt. Lett.* **38**, 1691 (2013).
- [20] H. Kim, T. C. Shen, K. Roy-Choudhury, G. S. Solomon, and E. Waks, *Phys. Rev. Lett.* **113**, 027403 (2014).
- [21] S. Unsleber, S. Maier, D. P. S. McCutcheon, Y. He, M. Dambach, M. Gschrey, N. Gregersen, J. Mørk, S. Reitzenstein, S. Höfling, C. Schneider, and M. Kamp, *Optica* **2**, 1072 (2015).
- [22] N. Akopian, N. H. Lindner, E. Poem, Y. Berlatzky, J. Avron, D. Gershoni, B. D. Gerardot, and P. M. Petroff, *Phys. Rev. Lett.* **96**, 130501 (2006).
- [23] M. Müller, S. Bounouar, K. D. Jöns, M. Glässl, and P. Michler, *Nat. Photonics* **8**, 224 (2014).
- [24] A. Dousse, J. Suffczyński, A. Beveratos, O. Krebs, A. Lemaître, I. Sagnes, J. Bloch, P. Voisin, and P. Senellart, *Nature (London)* **466**, 217 (2010).
- [25] H. Wang, H. Hu, T.-H. Chung, J. Qin, X. Yang, J.-P. Li, R.-Z. Liu, H.-S. Zhong, Y.-M. He, X. Ding, Y.-H. Deng, Q. Dai, Y.-H. Huo, S. Höfling, C.-Y. Lu, and J.-W. Pan, *Phys. Rev. Lett.* **122**, 113602 (2019).
- [26] X. Ding, Y. He, Z.-C. Duan, N. Gregersen, M.-C. Chen, S. Unsleber, S. Maier, C. Schneider, M. Kamp, S. Höfling, C.-Y. Lu, and J.-W. Pan, *Phys. Rev. Lett.* **116**, 020401 (2016).

- [27] P. K. Pathak and S. Hughes, *Phys. Rev. B* **82**, 045308 (2010).
- [28] J. Förstner, C. Weber, J. Danckwerts, and A. Knorr, *Phys. Rev. Lett.* **91**, 127401 (2003).
- [29] P. Kaer, T. R. Nielsen, P. Lodahl, A.-P. Jauho, and J. Mørk, *Phys. Rev. B* **86**, 085302 (2012).
- [30] A. Nazir and D. P. S. McCutcheon, *J. Phys.: Condens. Matter* **28**, 103002 (2016).
- [31] A. Carmele and S. Reitzenstein, *Nanophotonics* **8**, 655 (2019).
- [32] I. Wilson-Rae and A. Imamoglu, *Phys. Rev. B* **65**, 235311 (2002).
- [33] D. P. S. McCutcheon and A. Nazir, *New J. Phys.* **12**, 113042 (2010).
- [34] C. Roy and S. Hughes, *Phys. Rev. X* **1**, 021009 (2011).
- [35] A. Laucht, N. Hauke, J. M. Villas-Bôas, F. Hofbauer, G. Böhm, M. Kaniber, and J. J. Finley, *Phys. Rev. Lett.* **103**, 087405 (2009).
- [36] Y. Ota, S. Iwamoto, N. Kumagai, and Y. Arakawa, *Phys. Rev. Lett.* **107**, 233602 (2011).
- [37] D. Englund, A. Majumdar, A. Faraon, M. Toishi, N. Stoltz, P. Petroff, and J. Vučković, *Phys. Rev. Lett.* **104**, 073904 (2010).
- [38] S. Ates, S. M. Ulrich, A. Ulhaq, S. Reitzenstein, A. Löffler, S. Höfling, A. Forchel, and P. Michler, *Nat. Photonics* **3**, 724 (2009).
- [39] A. J. Bennett, J. P. Lee, D. J. P. Ellis, T. Meany, E. Murray, F. F. Floether, J. P. Griffiths, I. Farrer, D. A. Ritchie, and A. J. Shields, *Sci. Adv.* **2**, e1501256 (2016).
- [40] E. B. Flagg, A. Müller, S. V. Polyakov, A. Ling, A. Migdall, and G. S. Solomon, *Phys. Rev. Lett.* **104**, 137401 (2010).
- [41] S. Weiler, A. Ulhaq, S. M. Ulrich, D. Richter, M. Jetter, P. Michler, C. Roy, and S. Hughes, *Phys. Rev. B* **86**, 241304(R) (2012).
- [42] R. Oulton, J. J. Finley, A. I. Tartakovskii, D. J. Mowbray, M. S. Skolnick, M. Hopkinson, A. Vasanelli, R. Ferreira, and G. Bastard, *Phys. Rev. B* **68**, 235301 (2003).
- [43] Y.-S. Lee and S.-D. Lin, *Opt. Lett.* **39**, 6640 (2014).
- [44] M. Kaniber, A. Laucht, A. Neumann, J. M. Villas-Bôas, M. Bichler, M.-C. Amann, and J. J. Finley, *Phys. Rev. B* **77**, 161303(R) (2008).
- [45] A. Majumdar, M. Bajcsy, A. Rundquist, E. Kim, and J. Vučković, *Phys. Rev. B* **85**, 195301 (2012).
- [46] M. Minkov and V. Savona, *Phys. Rev. B* **87**, 125306 (2013).
- [47] M. Calic, C. Jarlov, P. Gallo, B. Dwir, A. Rudra, and E. Kapon, *Sci. Rep.* **7**, 4100 (2017).
- [48] J. K. Verma, H. Singh, and P. K. Pathak, *Phys. Rev. B* **98**, 125305 (2018).
- [49] J. K. Verma, H. Singh, and P. K. Pathak, *J. Opt. Soc. Am. B* **36**, 1200 (2019).
- [50] M. Glässl, A. M. Barth, K. Gawarecki, P. Machnikowski, M. D. Croitoru, S. Luker, D. E. Reiter, T. Kuhn, and V. M. Axt, *Phys. Rev. B* **87**, 085303 (2013).
- [51] S. Bounouar, M. Müller, A. M. Barth, M. Glässl, V. M. Axt, and P. Michler, *Phys. Rev. B* **91**, 161302(R) (2015).
- [52] M. Glässl, A. M. Barth, and V. M. Axt, *Phys. Rev. Lett.* **110**, 147401 (2013).
- [53] A. M. Barth, S. Luker, A. Vagov, D. E. Reiter, T. Kuhn, and V. M. Axt, *Phys. Rev. B* **94**, 045306 (2016).
- [54] C. Gustin and S. Hughes, *Phys. Rev. B* **98**, 045309 (2018).
- [55] C. Gustin and S. Hughes, *Adv. Quantum Technol.* **3**, 1900073 (2020).
- [56] P.-L. Ardel, L. Hanschke, K. A. Fischer, K. Müller, A. Kleinkauf, M. Koller, A. Bechtold, T. Simmet, J. Wierzbowski, H. Riedl, G. Abstreiter, and J. J. Finley, *Phys. Rev. B* **90**, 241404(R) (2014).
- [57] J. H. Quilter, A. J. Brash, F. Liu, M. Glässl, A. M. Barth, V. M. Axt, A. J. Ramsay, M. S. Skolnick, and A. M. Fox, *Phys. Rev. Lett.* **114**, 137401 (2015).
- [58] S. Hughes and H. J. Carmichael, *New J. Phys.* **15**, 053039 (2013).
- [59] T. Czerniuk, D. Wigger, A. V. Akimov, C. Schneider, M. Kamp, S. Höfling, D. R. Yakovlev, T. Kuhn, D. E. Reiter, and M. Bayer, *Phys. Rev. Lett.* **118**, 133901 (2017).
- [60] H. Kim, D. Sridharan, T. C. Shen, G. S. Solomon, and E. Waks, *Opt. Express* **19**, 2589 (2011).
- [61] A. Laucht, J. M. Villas-Bôas, S. Stobbe, N. Hauke, F. Hofbauer, G. Böhm, P. Lodahl, M.-C. Amann, M. Kaniber, and J. J. Finley, *Phys. Rev. B* **82**, 075305 (2010).
- [62] P. M. Vora, A. S. Bracker, S. G. Carter, M. Kim, C. S. Kim, and D. Gammon, *Phys. Rev. B* **99**, 165420 (2019).
- [63] K. Kamide, Y. Ota, S. Iwamoto, and Y. Arakawa, *Phys. Rev. A* **96**, 013853 (2017).
- [64] P. K. Pathak and S. Hughes, *Phys. Rev. B* **80**, 155325 (2009).
- [65] H. J. Sniijders, J. A. Frey, J. Norman, H. Flayac, V. Savona, A. C. Gossard, J. E. Bowers, M. P. van Exter, D. Bouwmeester, and W. Löffler, *Phys. Rev. Lett.* **121**, 043601 (2018).
- [66] P. Borri, W. Langbein, S. Schneider, U. Woggon, R. L. Sellin, D. Ouyang, and D. Bimberg, *Phys. Rev. Lett.* **87**, 157401 (2001).
- [67] S. M. Ulrich, S. Ates, S. Reitzenstein, A. Löffler, A. Forchel, and P. Michler, *Phys. Rev. Lett.* **106**, 247402 (2011).
- [68] K. Roy-Choudhury and S. Hughes, *Optica* **2**, 434 (2015).
- [69] D. P. S. McCutcheon and A. Nazir, *Phys. Rev. Lett.* **110**, 217401 (2013).
- [70] S. M. Tan, *J. Opt. B* **1**, 424 (1999).
- [71] M. Pleinert, J. von Zanthier, and G. S. Agarwal, *Optica* **4**, 779 (2017).
- [72] W. M. Pimenta, B. Marques, T. O. Maciel, R. O. Vianna, A. Delgado, C. Saavedra, and S. Pádua, *Phys. Rev. A* **88**, 012112 (2013).
- [73] F. Troiani, J. I. Perea, and C. Tejedor, *Phys. Rev. B* **74**, 235310 (2006).
- [74] G. Pfanner, M. Seliger, and U. Hohenester, *Phys. Rev. B* **78**, 195410 (2008).
- [75] G. Vidal and R. F. Werner, *Phys. Rev. A* **65**, 032314 (2002).
- [76] S. Ecker, F. Bouchard, L. Bulla, F. Brandt, O. Kohout, F. Steinlechner, R. Fickler, M. Malik, Y. Guryanova, R. Ursin, and M. Huber, *Phys. Rev. X* **9**, 041042 (2019).
- [77] S. Reitzenstein, A. Löffler, C. Hofmann, A. Kubanek, M. Kamp, J. P. Reithmaier, A. Forchel, V. D. Kulakovskii, L. V. Keldysh, I. V. Ponomarev, and T. L. Reinecke, *Opt. Lett.* **31**, 1738 (2006).
- [78] A. Dousse, L. Lanco, J. J. Suffczyński, E. Semenova, A. Miard, A. Lemaître, I. Sagnes, C. Roblin, J. Bloch, and P. Senellart, *Phys. Rev. Lett.* **101**, 267404 (2008).
- [79] A. Majumdar, M. Bajcsy, A. Rundquist, and J. Vučković, *Phys. Rev. Lett.* **108**, 183601 (2012).
- [80] S. Reitzenstein, C. Bockler, A. Löffler, S. Höfling, L. Worschech, A. Forchel, P. Yao, and S. Hughes, *Phys. Rev. B* **82**, 235313 (2010).